Floquet-heating-induced Bose condensation in a scarlike mode of an open driven optical-lattice system

Alexander Schnell [1,*] Ling-Na Wu,[1] Artur Widera [2] and André Eckardt [1]

[1]*Technische Universität Berlin, Institut für Theoretische Physik, 10623 Berlin, Germany*
[2]*Department of Physics and State Research Center OPTIMAS, University of Kaiserslautern-Landau, 67663 Kaiserslautern, Germany*

The combination of driving and dissipation guides a quantum system into a nonequilibrium steady state (NESS). It is an intriguing question, in how far this principle can be exploited for the robust preparation of interesting many-body target states beyond the strict constraints of thermal equilibrium. We consider an open system of ultracold bosonic atoms coupled to a heat bath and show that, counterintuitively, the interplay of bath-induced dissipation and controlled Floquet (i.e., driving-induced) heating can give rise to nonequilibrium Bose condensation in a quantum-scar-like mode protected from the drive. In particular, we use Floquet-Born-Markov theory to microscopically derive kinetic equations for a one-dimensional system of bosonic atoms in an optical lattice of finite extent coupled to a three-dimensional thermal bath of weakly interacting bosons treated in Bogoliubov theory. The bath temperature T is assumed to lie well above the crossover temperature, below which the majority of the system's particles form a (finite-size) Bose condensate in the single-particle ground state in equilibrium. However, when a strong local potential modulation is switched on, which resonantly excites the system, a nonequilibrium Bose condensate is formed in an excited state that decouples from the drive. This strategy of engineering the NESS of an open quantum system via tailored Floquet heating is likely to find applications also for different systems and target states.

I. INTRODUCTION

Floquet engineering is a powerful tool for controlling isolated quantum systems by means of time-periodic forcing [1–4]. Prominent examples include the control of phase transitions [5–9], the engineering of artificial magnetic fields and topological band structures in systems of charge-neutral particles such as atoms or photons [10–17], as well as the realization of so-called anomalous Floquet topological states that cannot exist in undriven systems [18–21]. Nevertheless, Floquet (i.e., periodically driven quantum) systems also suffer from heating, as it is caused by unwanted resonant excitation processes [22–28]. Such Floquet heating will generically guide an isolated system towards an infinite-temperature state, corresponding to eigenstate thermalization without energy conservation [29,30]. However, when a Floquet system is coupled to a bath [31–46], it will not approach infinite temperature, but a nonequilibrium steady state.

Previous work addressed the preparation of equilibriumlike states in open Floquet systems [47–51]. Here, we show that Floquet heating can be exploited for robust preparation of interesting nonequilibrium states. Namely, we consider a Bose gas in contact with a thermal bath of temperature well above the critical temperature and find that the heating induced by strong resonant driving can make the system Bose condense into an excited state, which is decoupled from the drive. In the following, we discuss this intriguing effect using a re-

alistic microscopic model describing a two-species mixture of ultracold atoms [52–65]. We solve this model numerically using kinetic equations and stochastic equations [36,39] based on Floquet-Born-Markov theory [31,32,34] and provide an intuitive explanation of the effect.

II. THE SYSTEM

We consider N noninteracting bosonic atoms in a one-dimensional (1D) optical lattice with strong transverse confinement, described by the tight-binding Hamiltonian

$$\hat{H}_0 = -J \sum_{i=1}^{M-1} (\hat{a}_{i+1}^\dagger \hat{a}_i + \hat{a}_i^\dagger a_{i+1}) = \sum_k \varepsilon_k \hat{b}_k^\dagger \hat{b}_k, \qquad (1)$$

with tunneling parameter J, number of lattice sites M (assuming box-type confinement), and annihilation operator $\hat{a}_i$ for a boson on site i. The eigenmodes, with annihilation operators $\hat{b}_k = \sum_i \langle \psi_k | i \rangle \hat{a}_i$, are characterized by wave functions $\langle i | \psi_k \rangle = \sqrt{2/(M+1)} \sin(kai)$ and energies $\varepsilon_k = -2J \cos(ka)$, with lattice spacing a and wave numbers $k = \nu \pi / [a(M+1)]$, with $\nu = 1, \ldots, M$. Additionally, the system is subjected to a local time-periodic potential modulation of amplitude A and frequency ω on site ℓ [see Fig. 1(a)], giving the total Hamiltonian

$$\hat{H}(t) = \hat{H}_0 + \hat{H}_D(t), \quad \hat{H}_D(t) = A[1 + \cos(\omega t)]\hat{a}_\ell^\dagger \hat{a}_\ell. \quad (2)$$

The box confinement and the local modulation can be realized using spatial light modulators. The single-particle Floquet states, $|\varphi_\alpha(t)\rangle = e^{-i\varepsilon_\alpha t/\hbar}|u_\alpha(t)\rangle$, labeled by $\alpha = 1, \ldots, M$, are
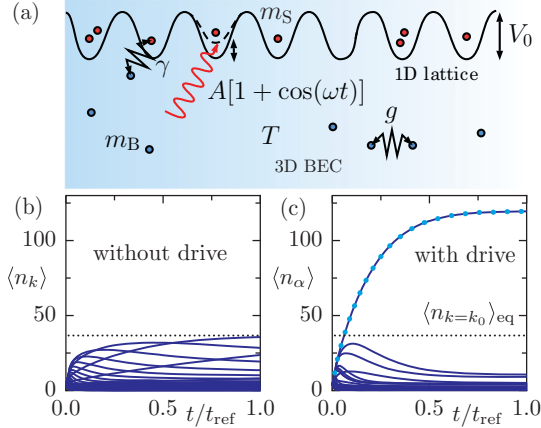
*schnell@tu-berlin.de

FIG. 1. (a) System: $N = 200$ noninteracting bosons in a 1D optical lattice of $M = 49$ sites subject to local time-periodic potential modulations of amplitude A, frequency $\hbar\omega = 1.5J$ at site $\ell = 20$. Bath: Weakly interacting 3D Bose condensate of temperature $T \approx 2.38J$ well above the crossover temperature $T_c^{\text{eq}} \approx 0.7J$ below which the majority of lattice bosons occupies the ground state in absence of driving. (b, c) Monte Carlo simulation of the relaxation dynamics of the mean occupations of (b) the single-particle eigenstates for the undriven system with $A = 0$ and (c) the single-particle Floquet states of the driven system with $A = J$. Statistical errors are smaller than the linewidth and therefore not shown. Dotted line, thermal ground-state occupation; blue bullets, occupation $\langle n_{k_c} \rangle$ of the undriven eigenstate $k_c = 2\pi/(\ell a)$.

characterized both by the quasienergies ε_α and the time-periodic Floquet modes $|u_\alpha(t)\rangle = |u_\alpha(t + \mathcal{T})\rangle$, with driving period $\mathcal{T} = 2\pi/\omega$. They are the eigenstates with eigenvalues $\exp(-i\varepsilon_\alpha \mathcal{T}/\hbar)$ of the single-particle one-cycle evolution operator from time t to $t + \mathcal{T}$. We also define the Floquet-mode annihilation operators $\hat{f}_\alpha = \sum_i \langle u_\alpha(t)|i\rangle \hat{a}_i$.

III. THE BATH

The system interacts weakly with a bath given by a weakly interacting three-dimensional Bose-Einstein condensate of another atomic species. The bath temperature lies well below the bath's critical temperature, but well above the crossover temperature T_c^{eq} below which the majority of lattice bosons occupies the ground state in absence of driving [see Fig. 1(a)]. Similar scenarios have recently been realized experimentally [52–59]. Approximating the bath as homogeneous with number density n_B over the extent of the lattice system and applying standard Bogoliubov theory [66], the bath Hamiltonian reads $\hat{H}_B = \sum_{\vec{q}} E_B(q)\hat{\beta}_{\vec{q}}^\dagger \hat{\beta}_{\vec{q}}$. Here $E_B(q) = \sqrt{E_0^2(q) + 2GE_0(q)}$ is the energy and $\hat{\beta}_{\vec{q}}$ the annihilation operator of a Bogoliubov quasiparticle with momentum $\hbar\vec{q}$, with $q = |\vec{q}|$, $E_0(q) = \hbar^2 q^2/(2m_B)$, bare mass m_B, $G = gn_B$, and intrabath contact interaction strength g.

The system particles interact with the bath particles via contact interactions of strength γ, described by $\hat{H}_{SB} = \gamma \int d^3\vec{r}\, \hat{n}_S(\vec{r})\hat{B}(\vec{r})$, and $\hat{B}(\vec{r}) = [\hat{n}_B(\vec{r}) - n_B]$, where $\hat{n}_S(\vec{r}) = \sum_{ij} w_i(\vec{r})w_j^*(\vec{r})\hat{a}_i^\dagger \hat{a}_j$, with Wannier function $w_i(\vec{r}) = \langle \vec{r}|i\rangle$ of lattice site i, describes the density of the system particles and $\hat{n}_B(\vec{r})$ the density of (bare) bath particles. Subtracting

the mean density n_B, corresponding to an irrelevant energy shift, ensures that $\text{Tr}_B(\hat{\varrho}_B\hat{H}_{SB}) = 0$, as required by the Born-Markov formalism [67]. The bath state is given by $\hat{\varrho}_B = \exp(-\hat{H}_B/T)/Z_B$ (with $k_B \equiv 1$). In leading (linear) order with respect to the Bogoliubov modes (describing single-phonon scattering, which is dominant for low bath temperatures [60]), $\hat{B}(\vec{r}) \simeq \sqrt{n_B/V} \sum_{\vec{q}\neq\vec{0}} e^{i\vec{q}\cdot\vec{r}}[u_q\hat{\beta}_{\vec{q}} - v_q\hat{\beta}_{-\vec{q}}^\dagger]$, where u_q and v_q, with $u_q^2 - v_q^2 = 1$ and $2u_q v_q = G/E_B(q)$, are the usual Bogoliubov coefficients [67].

We assume ultraweak system-bath coupling, which is small compared to all single-particle (quasi)energy splittings in the system (so that also bath-mediated interactions are negligible). Under this assumption, we derive a master equation using Floquet-Born-Markov theory in secular approximation [32–34,68–70]. Then, the off-diagonal matrix elements of the density matrix ρ in Floquet-state representation decouple from the diagonal ones and decay rapidly [33,34,69], so that $\hat{\varrho}(t) \simeq \sum_{\mathbf{n}} p_{\mathbf{n}}(t)|\mathbf{n}\rangle\langle\mathbf{n}|$, where $p_{\mathbf{n}}(t)$ is the probability of the system being in the many-body Floquet state $|\mathbf{n}\rangle = |\mathbf{n}(t)\rangle = |\mathbf{n}(t + \mathcal{T})\rangle$, characterized by the vector of occupation numbers $\mathbf{n} = (n_1, \ldots, n_M)$ for single-particle Floquet modes $|u_\alpha(t)\rangle$. The probabilities follow the classical many-body rate equation [39]

$$\dot{p}_{\mathbf{n}}(t) = \sum_{\alpha\beta}(1 + n_\beta)n_\alpha[R_{\alpha\beta}p_{\mathbf{n}_{\alpha\leftarrow\beta}}(t) - R_{\beta\alpha}p_{\mathbf{n}}(t)], \quad (3)$$

where $\mathbf{n}_{\alpha\leftarrow\beta}$ are occupation numbers obtained from $\mathbf{n}$ by transferring a particle from mode β to α and $R_{\alpha\beta}$ denotes the corresponding Fermi's "golden rule" type of single-particle rate:

$$R_{\alpha\beta} = \frac{2\pi\gamma^2}{\hbar} \sum_{K\in\mathbb{Z}} \sum_{ij} (v_i)_{\alpha\beta}^{(K)*}(v_j)_{\alpha\beta}^{(K)} W_{ij}\big(\Delta_{\alpha\beta}^{(K)}\big). \quad (4)$$

Here $(v_i)_{\alpha\beta}^{(K)} = \mathcal{T}^{-1}\int_0^{\mathcal{T}} dt\, e^{-iK\omega t}\langle u_\alpha(t)|i\rangle\langle i|u_\beta(t)\rangle$ are matrix elements and $W_{ij}(E) = J_{ij}(E)/(e^{E/T} - 1)$ bath correlation functions, with spectral densities $J_{ij}(E) = \text{sgn}(E)n_B q(E)^3 I_{ij}[q(E)]/(8\pi^2\sqrt{E^2 + G^2})$, wave number $q(E)$ for a bath quasiparticle with energy E, and $I_{ij}(q) \approx e^{-\frac{1}{2}q^2 d^2}2\text{sinc}[qa(i - j)]$ (obtained by approximating Wannier functions by oscillator ground states with isotropic oscillator length d) [67].

Equation (3) describes exponentially many probabilities $p_{\mathbf{n}}(t)$, but single- and few-particle expectation values, like $\langle \hat{n}_\alpha\rangle(t)$ or $\langle \hat{n}_\alpha\hat{n}_\beta\rangle(t)$ with $\hat{n}_\alpha = \hat{f}_\alpha^\dagger\hat{f}_\alpha$, can be obtained efficiently by quantum-jump Monte Carlo simulations [71], i.e., by sampling over random walks (trajectories) between different Fock states $|\mathbf{n}\rangle$ [39]. This method gives quasiexact results, in the sense that the accuracy is controlled by the number of trajectories. Alternatively, we can obtain $\langle \hat{n}_\alpha\rangle(t)$ from the equations of motion [36,39,72] $d\langle \hat{n}_\alpha\rangle/dt = \sum_\beta[R_{\alpha\beta}\langle(\hat{n}_\alpha + 1)\hat{n}_\beta\rangle - R_{\beta\alpha}\langle(\hat{n}_\beta + 1)\hat{n}_\alpha\rangle]$. These depend, however, on two-body correlations $\langle \hat{n}_\alpha\hat{n}_\beta\rangle$, which reflects that, even though we assume vanishing intrasystem interactions, we are still dealing with an interacting problem, since the coupling operator $\hat{H}_{SB}$ is cubic in the system and bath (quasiparticle) operators. We obtain a closed set of nonlinear kinetic equations for the mean occupations $\langle \hat{n}_\alpha\rangle(t)$ by additionally making the mean-field approximation $\langle \hat{n}_\alpha\hat{n}_\beta\rangle \approx \langle \hat{n}_\alpha\rangle\langle \hat{n}_\beta\rangle$ (corresponding to
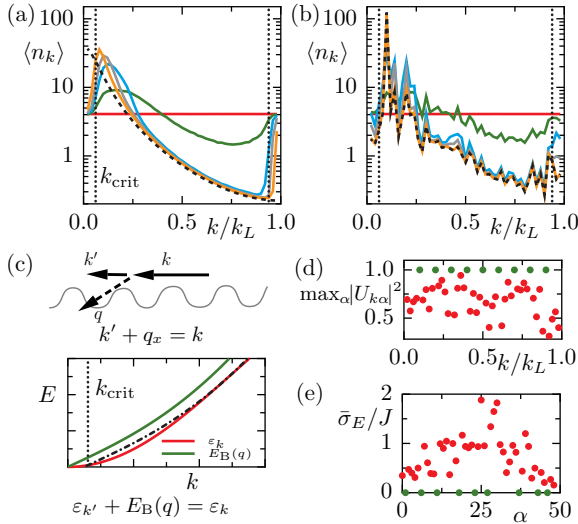
FIG. 2. (a, b) Snapshots of the momentum distribution $\langle n_k \rangle$ corresponding to Figs. 1(b) and 1(c), respectively, at times $t/t_{ref} = 0, 0.01, 0.05, 0.2, 1$ (red, green, blue, gray, orange). Dashed line, steady-state distribution inferred from the mean-field theory; dotted lines, critical momenta k_{crit} below (above) which one-phonon scattering is suppressed in the undriven case. (c) Top: Collision leading to the emission of a bath phonon. Bottom: Bogoliubov dispersion of the bath (green) and lattice dispersion (red). Only after shifting the bath dispersion (dash dotted) by $k' \geqslant k_{crit}$ there are multiple intersections. (d) Largest overlap $U_{k\alpha} = \langle \psi_k | u_\alpha(0) \rangle$ between the eigenstates k of the undriven and the Floquet states α of the driven system. (e) Cycle-averaged standard deviation $\bar{\sigma}_E^2 = \mathcal{T}^{-1} \int_0^{\mathcal{T}} \langle u_\alpha(t) | \hat{H}^2(t) | u_\alpha(t) \rangle dt - E_{avg,\alpha}^2$ of the energy $E_{avg,\alpha} = \mathcal{T}^{-1} \int_0^{\mathcal{T}} \langle u_\alpha(t) | \hat{H}(t) | u_\alpha(t) \rangle dt$ of the Floquet mode α. (d, e) Undriven modes colored green.

a Gaussian ansatz for the system state) [39,67]. In the following, we mainly show exact Monte Carlo solutions of Eq. (3). However, when scanning large parameter spaces for steady states, we employ also the kinetic equations, which still provide an excellent approximation. This can be seen from Fig. 2(b), where the orange solid line, showing the late-time momentum distribution of the driven system, agrees very well with the black dashed line, giving the steady-state prediction of the kinetic theory.

IV. PARAMETERS

Inspired by recent experiments [52–58], we assume $N = 200$ bosonic ^{39}K atoms on $M = 49$ lattice sites immersed in a bath of ^{87}Rb (and discuss results for Cs in Rb in the Supplemental Material [67]). We consider a lattice depth of $V_0 = 6E_R$, with recoil energy $E_R = \hbar^2 k_L^2/(2m_S)$, potassium mass m_S, lattice momentum $k_L = \pi/a$, and lattice spacing $a = 395.01$ nm corresponding to the Rb tune-out wavelength of 790.01 nm [73,74]. For convenience, the lattice minima are considered to be isotropic, which slightly underestimates the transverse confinement. Moreover, the bath particles interaction parameter reads $G = gn_B = 0.05E_R$ (corresponding to $g = 2\pi\hbar^2 a_{Rb}/m_B$, $a_{Rb} = 104$ Bohr radii, and $n_B = 6.29/a^3$). Within our theoretical framework, the system-bath coupling γ enters through the time scale $t_{ref} = 16\pi\hbar^3/(m_B k_L n_B \gamma^2)$ of the relaxation dynamics. In an experiment $\gamma = 2\pi\hbar^2 a_{SB}/\tilde{m}$ is

given by the K-Rb scattering length a_{SB} and reduced mass $\tilde{m}$. The bath possesses the temperature $T = 2.38J$, corresponding to 15% of its estimated critical temperature $T_c^{Bath} = 15.9J$, and the system is initialized in an infinite-temperature state (within the lowest band), with all Floquet and eigenmodes populated equally.

V. RELAXATION DYNAMICS OF THE UNDRIVEN SYSTEM

Let us first discuss the equilibration dynamics of the undriven system, $A = 0$. Here the Floquet modes and quasienergies equal the single-particle eigenstates of $\hat{H}_0$ and their energies. In Fig. 1(b) we show the time evolution of their mean occupations $\langle \hat{n}_k \rangle = \langle \hat{b}_k^\dagger \hat{b}_k \rangle$ using the Monte Carlo simulations. Since the system is one-dimensional, equilibrium Bose condensation is a finite-size effect. The corresponding crossover temperature, below which the majority of bosons occupies the single-particle ground state and the coherence length exceeds the system extent, can be estimated as $T_c^{eq} \approx 8.3JN/M^2 \approx 0.69J$ [67,75]. As the bath temperature $T = 2.38J$ lies above this crossover temperature, at equilibrium, Bose condensation is not expected. This is confirmed in Fig. 1(b), where the dotted line indicates the thermal occupation of the ground state, which is approached in the long-time limit.

We, moreover, observe that a rather fast dynamics for $t \lesssim 0.1t_{ref}$ is followed by very slow relaxation taking much longer than t_{ref}. The reason for this separation of time scales becomes apparent from Fig. 2(a) where we depict snapshots of the distribution $\langle \hat{n}_k \rangle$ at intermediate times t (solid lines) and compare them to the equilibrium distribution at the bath temperature (dashed line). Below (above) the critical wave numbers k_{crit} ($k_L - k_{crit}$) the absorption or emission of bath excitations is strongly suppressed, since in an infinite system it would not be possible to conserve both energy and momentum in such a process. Namely, for a transition $k \to k'$, the absolute value of the quasiparticle momentum obeys $q > |q_x| = |k - k'|$ [see Fig. 2(c)] [76], corresponding to quasiparticle energies $E_B(q) \geqslant E_B(|k - k'|)$ that have to match $|\varepsilon_k - \varepsilon_{k'}|$, which is impossible for too small or too large k'. This is illustrated in Fig. 2(c): Only after shifting the Bogoliubov dispersion $E_B(q)$ (green line) from the origin to the point $(k_{crit}, \varepsilon_{k_{crit}})$ (dashed-dotted line) or further to $k' \geqslant k_{crit}$, there is more than one intersection with the lattice dispersion of the system ε_k (red line) where, for the corresponding k', k energy and momentum conservation can be fulfilled. Similar behavior has been found for a free impurity immersed in a superfluid [60] (where such a critical momentum only exists for $m_S > m_B$). Since for the finite lattice of M sites momentum is conserved only approximately, ultimately, for $t \gg t_{ref}$, the system thermalizes with temperature T.

VI. DRIVEN-DISSIPATIVE SYSTEM

We now turn to the dynamics of the driven system with driving amplitude $A = J$, frequency $\hbar\omega = 1.5J$, and position $\ell = 20$. Unlike in the typical regime of Floquet engineering, the driving frequency is *not* large compared to the system's bandwidth $4J$. Thus, driving-induced heating via resonant excitation [77] is not suppressed, but a dominant impact of

the drive. In Fig. 1(c) we depict the evolution of the mean occupations of the Floquet modes α on the same time interval as in Fig. 1(b). We can observe that, in contrast to the undriven scenario, the system quickly relaxes to a steady state on a time $t \lesssim t_{\text{ref}}/2$. This is not surprising, since the local driving potential breaks both energy and approximate momentum conservation, which suppress the relaxation in the undriven case.

However, the most striking effect is that in the presence of driving the system approaches a nonequilibrium steady state, where more than 60% of the particles form a nonequilibrium Bose condensate by occupying the same single-particle Floquet state. Remarkably, this effect happens despite the Floquet (i.e., driving-induced) heating. In fact we will argue below that it is actually the interplay between the driving-induced heating and the dissipation from the bath, which causes the nonequilibrium condensation. In Fig. 2(b) we plot snapshots of the mean occupations $\langle \hat{n}_k \rangle$ of the undriven eigenmodes and we can see that the condensate occurs in a state having a large overlap with the excited undriven eigenstate $|\psi_{k_c}\rangle$ with wave number $k_c = 2\pi/(\ell a)$. Plotting the occupation of this mode as blue bullets in Fig. 1(c), we can see that it perfectly matches the occupation of the most populated Floquet mode, indicating that both modes are in fact identical. This leads us to the following intuitive explanation of the at first glance counterintuitive effect.

The mode k_c possesses a node at lattice site ℓ. It is the lowest-energy state of a series of modes $k_\nu = \nu 2\pi/(\ell a)$, with $\nu = 1, 2, \ldots, M-1$, which decouple from the drive, since $\sin(k_\nu a\ell) = 0$. These undriven eigenstates remain Floquet states of the driven system, as can be inferred from Fig. 2(d), where we plot for each undriven mode k its maximum overlap $\max_\alpha |\langle \psi_k | u_\alpha(0) \rangle|^2$ with a Floquet mode α. We can clearly see that the k_ν, which are colored green, correspond to Floquet modes of the problem. In Fig. 2(e) we plot the (period-averaged) standard deviation of the energy of each Floquet mode α. As a result of the strong and resonant driving, almost all modes are well delocalized in energy, except for those Floquet states corresponding to the undriven modes k_ν (green bullets), which possess sharp energies. We can conclude that the undriven modes k_ν play a role very similar to quantum many-body-scar states [78–80]. In a quantum many-body system, where the majority of states follows the eigenstate thermalization hypothesis (ETH), so that they give rise to thermal expectation values, such many-body scars correspond to a small set of nonergodic quantum states violating the ETH. In a many-body Floquet system, a generic Floquet state is completely delocalized in energy, corresponding to an infinite-temperature state [29,30]. The Floquet modes $|u_\alpha(t)\rangle$ of our system are single-particle states of a finite system and, thus, cannot be expected to provide infinite-temperature expectation values. Nevertheless, we can clearly see that they are broad in energy, while, in stark contrast, the undriven modes k_ν have sharp energies and, in this sense, resemble quantum many-body scars [81]. It is an interesting open question, though, whether these scarlike single-particle modes can be related or generalized to actual quantum-many-body scars in large interacting systems.

We can now divide the system into two parts, given by the minority of undriven scarlike modes k_ν, which are local and
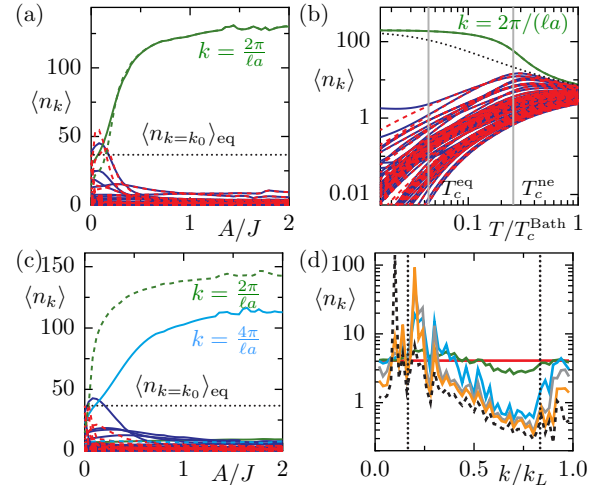

FIG. 3. Mean-field solutions for mean occupations $\langle n_k \rangle$ of quasi-momenta k vs (a) driving strength A and (b) bath temperature T for $t \to \infty$ (dashed lines) and $t = t_{\text{ref}}$ (solid lines). Dotted line, thermal ground-state occupation. Parameter as in Fig. 1(c), where $G = 0.05E_R$. (c) Like (a) but for increased intrabath iterations $G = 0.1E_R$. At $t = t_{\text{ref}}$ a metastable condensate is formed in the mode $k = 4\pi/(\ell a)$. (d) Like Fig. 2(b) but for $G = 0.1E_R$.

well separated in energy, on the one hand, and the majority of "actual" Floquet states on the other. As a consequence of the large level splitting, within the undriven subspace the bath will efficiently transport particles to the lowest state, k_c. Moreover, among the driven states the mixing of low-energy with more excited states raises their energies on average, corresponding to Floquet heating, so that, as a result, we find also an enhanced bath-induced transfer from driven modes towards k_c (this might be viewed as a Floquet-heating-induced thermoelectric effect). Both effects together then lead to the observed nonequilibrium Bose condensation in the excited state k_c.

A somewhat related but in its origin rather different effect can be observed, when instead of being driving periodically the system is coupled to a very hot local bath [75]. However, in stark contrast to the driven system, in this scenario the eigenstate structure of the system is not altered at all. Moreover, the experimental realization of a local drive is much easier than that of an additional hot local bath.

The nonequilibrium condensation does not rely on fine tuning. We equally find it for caesium atoms in a rubidium bath [67]. In Fig. 3 we also investigate its dependence on both the driving strength A/J [Fig. 3(a)] and the bath temperature T/T_c^{bath} [Fig. 3(b)] by plotting $\langle \hat{n}_k \rangle$ at time $t/t_{\text{ref}} = 1$ (solid line) and in the steady state (dashed lines) (the dotted line is the equilibrium ground-state occupation). The majority of particles occupies a single mode for $A/J \gtrsim 0.5$ [Fig. 3(a)] and $T \lesssim T_c^{\text{ne}} = JN/M \approx 4J \gg T_c^{\text{eq}} \approx 0.69J$ [Fig. 3(b)]. Here T_c^{ne} denotes a rough estimate of the nonequilibrium condensation temperature below which half the particles occupy k_c. It is obtained by assuming that within the cold undriven modes the large level splitting causes the bath to transport all particles to k_c, while the remaining N' particles are equally distributed over the driven modes. T_c^{ne} then results from setting $N' = N/2$

and approximating the coupling between driven and undriven modes by nonresonant ($K = 0$) transitions [67].

VII. TRANSIENT CONDENSATION

Also for the driven system the relaxation is slower for $k < k_{\text{crit}}$. When $k_c < k_{\text{crit}} < k_2$ (which can be achieved by increasing G/E_R to 0.1, e.g., via the bath density n_B), we observe that during the evolution first the undriven mode $k_2 = 2k_c = 4\pi/(\ell a)$ acquires a large occupation [see Figs. 3(c) and 3(d)]. However, ultimately the system relaxes to its true steady state with a condensate in $k = k_c$ (dashed lines).

VIII. CONCLUSIONS

We have described a mechanism for the controlled preparation of nonequilibrium steady states. It relies on the combination of bath-induced dissipation and the driving-induced engineering of scarlike quantum modes that, unlike all other Floquet modes, do not suffer from Floquet heating. Using realistic parameters for a system of bosonic atoms in an optical lattice, we have demonstrated the preparation of an excited-state Bose condensate for bath temperatures well above the equilibrium condensation temperature. It will be interesting to explore the construction of similar condensates for the preparation of correlated target states of interacting systems.

[1] N. Goldman and J. Dalibard, Phys. Rev. X **4**, 031027 (2014).

[2] M. Bukov, L. D'Alessio, and A. Polkovnikov, Adv. Phys. **64**, 139 (2015).

[3] A. Eckardt, Rev. Mod. Phys. **89**, 011004 (2017).

[4] T. Oka and S. Kitamura, Annu. Rev. Condens. Matter Phys. **10**, 387 (2019).

[5] A. Eckardt, C. Weiss, and M. Holthaus, Phys. Rev. Lett. **95**, 260404 (2005).

[6] A. Zenesini, H. Lignier, D. Ciampini, O. Morsch, and E. Arimondo, Phys. Rev. Lett. **102**, 100403 (2009).

[7] J. Struck, M. Weinberg, C. Ölschläger, P. Windpassinger, J. Simonet, K. Sengstock, R. Höppner, P. Hauke, A. Eckardt, M. Lewenstein, and L. Mathey, Nat. Phys. **9**, 738 (2013).

[8] C. Sträter and A. Eckardt, Phys. Rev. A **91**, 053602 (2015).

[9] B. Song, S. Dutta, S. Bhave, J.-C. Yu, E. Carter, N. Cooper, and U. Schneider, Nat. Phys. **18**, 259 (2022).

[10] T. Oka and H. Aoki, Phys. Rev. B **79**, 081406(R) (2009).

[11] M. Aidelsburger, M. Atala, S. Nascimbène, S. Trotzky, Y.-A. Chen, and I. Bloch, Phys. Rev. Lett. **107**, 255301 (2011).

[12] J. Struck, C. Ölschläger, M. Weinberg, P. Hauke, J. Simonet, A. Eckardt, M. Lewenstein, K. Sengstock, and P. Windpassinger, Phys. Rev. Lett. **108**, 225304 (2012).

[13] M. Aidelsburger, M. Atala, M. Lohse, J. T. Barreiro, B. Paredes, and I. Bloch, Phys. Rev. Lett. **111**, 185301 (2013).

[14] M. C. Rechtsman, J. M. Zeuner, Y. Plotnik, Y. Lumer, D. Podolsky, F. Dreisow, S. Nolte, M. Segev, and A. Szameit, Nature (London) **496**, 196 (2013).

[15] G. Jotzu, M. Messer, T. U. Rémi Desbuquois, Martin Lebrat, D. Greif, and T. Esslinger, Nature (London) **515**, 237 (2014).

[16] M. E. Tai, A. Lukin, M. Rispoli, R. Schittko, T. Menke, D. Borgnia, P. M. Preiss, F. Grusdt, A. M. Kaufman, and M. Greiner, Nature (London) **546**, 519 (2017).

[17] B. Wang, F. N. Ünal, and A. Eckardt, Phys. Rev. Lett. **120**, 243602 (2018).

[18] T. Kitagawa, E. Berg, M. Rudner, and E. Demler, Phys. Rev. B **82**, 235114 (2010).

[19] M. S. Rudner, N. H. Lindner, E. Berg, and M. Levin, Phys. Rev. X **3**, 031005 (2013).

[20] L. J. Maczewsky, J. M. Zeuner, S. Note, and A. Szameit, Nat. Commun. **8**, 13756 (2017).

[21] K. Wintersperger, C. Braun, F. N. Ünal, A. Eckardt, M. Di Liberto, N. Goldman, I. Bloch, and M. Aidelsburger, Nat. Phys. **16**, 1058 (2020).

[22] M. Weinberg, C. Ölschläger, C. Sträter, S. Prelle, A. Eckardt, K. Sengstock, and J. Simonet, Phys. Rev. A **92**, 043621 (2015).

[23] D. A. Abanin, W. De Roeck, and F. Huveneers, Phys. Rev. Lett. **115**, 256803 (2015).

[24] T. Bilitewski and N. R. Cooper, Phys. Rev. A **91**, 063611 (2015).

[25] C. Sträter and A. Eckardt, Z. Naturforsch. **71**, 909 (2016).

[26] M. Reitter, J. Näger, K. Wintersperger, C. Sträter, I. Bloch, A. Eckardt, and U. Schneider, Phys. Rev. Lett. **119**, 200402 (2017).

[27] G. Sun and A. Eckardt, Phys. Rev. Research **2**, 013241 (2020).

[28] K. Viebahn, J. Minguzzi, K. Sandholzer, A.-S. Walter, M. Sajnani, F. Görg, and T. Esslinger, Phys. Rev. X **11**, 011057 (2021).

[29] L. D'Alessio and M. Rigol, Phys. Rev. X **4**, 041048 (2014).

[30] A. Lazarides, A. Das, and R. Moessner, Phys. Rev. E **90**, 012110 (2014).

[31] R. Blümel, A. Buchleitner, R. Graham, L. Sirko, U. Smilansky, and H. Walther, Phys. Rev. A **44**, 4521 (1991).

[32] S. Kohler, T. Dittrich, and P. Hänggi, Phys. Rev. E **55**, 300 (1997).

[33] H.-P. Breuer, W. Huber, and F. Petruccione, Phys. Rev. E **61**, 4883 (2000).

[34] D. W. Hone, R. Ketzmerick, and W. Kohn, Phys. Rev. E **79**, 051129 (2009).

[35] R. Ketzmerick and W. Wustmann, Phys. Rev. E **82**, 021114 (2010).

[36] D. Vorberg, W. Wustmann, R. Ketzmerick, and A. Eckardt, Phys. Rev. Lett. **111**, 240405 (2013).

[37] M. Langemeyer and M. Holthaus, Phys. Rev. E **89**, 012101 (2014).

[38] K. Szczygielski, J. Math. Phys. **55**, 083506 (2014).

[39] D. Vorberg, W. Wustmann, H. Schomerus, R. Ketzmerick, and A. Eckardt, Phys. Rev. E **92**, 062119 (2015).

[40] F. Haddadfarshi, J. Cui, and F. Mintert, Phys. Rev. Lett. **114**, 130402 (2015).

[41] C. M. Dai, Z. C. Shi, and X. X. Yi, Phys. Rev. A **93**, 032121 (2016).

[42] T. Shirai, J. Thingna, T. Mori, S. Denisov, P. Hänggi, and S. Miyashita, New J. Phys. **18**, 053008 (2016).

[43] S. Restrepo, J. Cerrillo, V. M. Bastidas, D. G. Angelakis, and T. Brandes, Phys. Rev. Lett. **117**, 250401 (2016).

[44] A. Schnell, A. Eckardt, and S. Denisov, Phys. Rev. B **101**, 100301(R) (2020).

[45] T. N. Ikeda, K. Chinzei, and M. Sato, SciPost Phys. Core **4**, 033 (2021).

[46] A. Schnell, S. Denisov, and A. Eckardt, Phys. Rev. B **104**, 165414 (2021).

[47] T. Shirai, T. Mori, and S. Miyashita, Phys. Rev. E **91**, 030101(R) (2015).

[48] H. Dehghani, T. Oka, and A. Mitra, Phys. Rev. B **91**, 155422 (2015).

[49] K. I. Seetharam, C.-E. Bardyn, N. H. Lindner, M. S. Rudner, and G. Refael, Phys. Rev. X **5**, 041050 (2015).

[50] T. Iadecola, T. Neupert, and C. Chamon, Phys. Rev. B **91**, 235133 (2015).

[51] T. Qin, A. Schnell, K. Sengstock, C. Weitenberg, A. Eckardt, and W. Hofstetter, Phys. Rev. A **98**, 033601 (2018).

[52] N. Spethmann, F. Kindermann, S. John, C. Weber, D. Meschede, and A. Widera, Phys. Rev. Lett. **109**, 235301 (2012).

[53] M. Hohmann, F. Kindermann, T. Lausch, D. Mayer, F. Schmidt, E. Lutz, and A. Widera, Phys. Rev. Lett. **118**, 263401 (2017).

[54] F. Schmidt, D. Mayer, T. Lausch, D. Adam, Q. Bouton, M. Hohmann, F. Kindermann, J. Koch, J. Nettersheim, and A. Widera, Phys. Status Solidi B **256**, 1800710 (2019).

[55] Q. Bouton, J. Nettersheim, D. Adam, F. Schmidt, D. Mayer, T. Lausch, E. Tiemann, and A. Widera, Phys. Rev. X **10**, 011018 (2020).

[56] F. Schmidt, D. Mayer, Q. Bouton, D. Adam, T. Lausch, N. Spethmann, and A. Widera, Phys. Rev. Lett. **121**, 130403 (2018).

[57] F. Schmidt, D. Mayer, Q. Bouton, D. Adam, T. Lausch, J. Nettersheim, E. Tiemann, and A. Widera, Phys. Rev. Lett. **122**, 013401 (2019).

[58] A. Mil, T. V. Zache, A. Hegde, A. Xia, R. P. Bhatt, M. K. Oberthaler, P. Hauke, J. Berges, and F. Jendrzejewski, Science **367**, 1128 (2020).

[59] B. Zhu, S. Häfner, B. Tran, M. Gerken, J. Ulmanis, E. Tiemann, and M. Weidemüller, High partial-wave feshbach resonances in an ultracold ^{6}Li - ^{133}Cs mixture, arXiv:1912.01264.

[60] T. Lausch, A. Widera, and M. Fleischhauer, Phys. Rev. A **97**, 023621 (2018).

[61] R. G. Lena and A. J. Daley, Phys. Rev. A **101**, 033612 (2020).

[62] A. Klein, M. Bruderer, S. R. Clark, and D. Jaksch, New J. Phys. **9**, 411 (2007).

[63] P. Ostmann and W. T. Strunz, Cooling and frequency shift of an impurity in a ultracold Bose gas using an open system approach, arXiv:1707.05257 (2017).

[64] T. Lausch, A. Widera, and M. Fleischhauer, Phys. Rev. A **97**, 033620 (2018).

[65] S. Rammohan, A. K. Chauhan, R. Nath, A. Eisfeld, and S. Wüster, Phys. Rev. A **103**, 063307 (2021).

[66] C. J. Pethick and H. Smith, *Bose-Einstein Condensation in Dilute Gases*, 2nd ed. (Cambridge University, Cambridge, England, 2008).

[67] See Supplemental Material at http://link.aps.org/supplemental/10.1103/PhysRevA.107.L021301 for details on the bath Hamiltonian and the system-bath coupling; the Floquet-Born-Markov-secular approximation; the condensation temperature in equilibrium; the non-equilibrium condensation temperature; and results with parameters for Caesium in Rubidium.

[68] H. Breuer and F. Petruccione, *The Theory of Open Quantum Systems* (Oxford University, New York, 2002).

[69] W. Wustmann, Statistical mechanics of time-periodic quantum systems, Ph.D. thesis, TU Dresden, 2010.

[70] O. R. Diermann and M. Holthaus, Sci. Rep. **9**, 17614 (2019).

[71] M. B. Plenio and P. L. Knight, Rev. Mod. Phys. **70**, 101 (1998).

[72] A. Schnell, R. Ketzmerick, and A. Eckardt, Phys. Rev. E **97**, 032136 (2018).

[73] L. J. LeBlanc and J. H. Thywissen, Phys. Rev. A **75**, 053612 (2007).

[74] F. Schmidt, D. Mayer, M. Hohmann, T. Lausch, F. Kindermann, and A. Widera, Phys. Rev. A **93**, 022507 (2016).

[75] A. Schnell, D. Vorberg, R. Ketzmerick, and A. Eckardt, Phys. Rev. Lett. **119**, 140602 (2017).

[76] Umklapp scattering is included in the argument because the dispersion $\varepsilon_{k'}$ is unchanged under $k' \to k' + k_L$.

[77] A. Eckardt and E. Anisimovas, New J. Phys. **17**, 093039 (2015).

[78] M. Serbyn, D. A. Abanin, and Z. Papić, Nat. Phys. **17**, 675 (2021).

[79] S. Moudgalya, B. A. Bernevig, and N. Regnault, Rep. Prog. Phys. **85**, 086501 (2022).

[80] A. Chandran, T. Iadecola, V. Khemani, and R. Moessner, Annu. Rev. Condens. Matter Phys. **14** (2022).

[81] We avoid the term "quantum scar," without the attribute "many-body," since this term was coined specifically for quantum states related to unstable periodic orbits in a corresponding classical model.